Environment International 196 (2025) 109265

Contents lists available at ScienceDirect

Environment International

journal homepage: www.elsevier.com/locate/envint

Full length article

Street-scale black carbon modelling over the West Midlands, United Kingdom: Sensitivity test of traffic emission factor adjustments

Jian Zhong [a,d], Yinghua Li [a,b], William James Bloss [a], Roy M. Harrison [a,c,*]

[a] School of Geography, Earth & Environmental Sciences, University of Birmingham, Edgbaston, Birmingham B15 2TT, UK
[b] School of Resource and Environment Engineering, Jilin Institute of Chemical Technology, 132022, China
[c] Department of Environmental Sciences/Center of Excellence in Environmental Studies, King Abdulaziz University, PO Box 80203, Jeddah 21589, Saudi Arabia
[d] Computational Science and Engineering Group, Centre for Advanced Simulation and Modelling, University of Greenwich, London, SE10 9LS, UK

ARTICLE INFO

Handling editor: Xavier Querol

Keywords:
Black Carbon
Air Quality Modelling
Traffic Emission Factors
ADMS-Urban

ABSTRACT

Black carbon is harmful for climate, environment, and human health. Road traffic is one of the major sources for black carbon in urban areas. This study develops a street scale air quality model configuration for the dispersion of black carbon concentrations across the West Midlands, UK, incorporating updated road traffic emission factors. A range of modelling cases accounting for traffic emission factor adjustments was conducted and evaluated against measurements at three monitoring sites within the region. The model overall has good performance. With unadjusted traffic emission factors, the model can capture black carbon annual concentrations at urban background sites. However, an adjustment (factor of 3) for the traffic emission factors is needed to better represent the roadside site (although with a slight overestimation of 3 % in annual concentration). There are near-linear relationships between black carbon concentrations and the adjustment ratio for the traffic emission factor. Black carbon concentration maps have been generated at 10 m × 10 m resolution, which were then aggregated into health-related electoral ward and local authority levels.

1. Introduction

Black carbon is an important component of Particulate Matter (PM), mainly generated from the incomplete combustion of fuels and biomass (Bond et al., 2013). Many studies have focused on black carbon due to its negative impact on climate, environment, and public health in recent decades. Black carbon is a unique short-lived climate pollutant that has played a very important role in the global climate system since pre-industrial times (Koch et al., 2009). The “direct effect” is that black carbon in the atmosphere can absorb incoming solar radiation, and release it as heat in the lower atmosphere causing global warming (Ramanathan and Carmichael, 2008). The “albedo effect” occurs when black carbon is deposited in snow or ice-covered areas, which darkens the surface, absorbs more incoming solar radiation and leads to faster snow or ice melt (Réveillet et al., 2021, Eckhardt et al., 2023, Kang et al., 2020). The “semi-direct effect” is that black carbon can influence cloud formation via the changes in atmospheric stability or relative humidity (Johnson et al., 2004). Black carbon may also have an “indirect effect” for cloud condensation by acting as ice nuclei (Oshima et al., 2009, Liu et al., 2009). Black carbon is also responsible for environmental impacts leading to visibility reduction (Li et al., 2022) and poor air quality (Healy et al., 2019, Yang et al., 2022). Compared with mass concentrations such as $PM_{2.5}$ and PM_{10}, black carbon has been suggested as a more reliable indicator for assessing the health risks of ambient particles (Janssen et al., 2011). Black carbon concentrations are found to be significantly associated with asthma symptoms in toxicological and epidemiological studies (Jung et al., 2017, Hansel et al., 2018). Black carbon has a close relationship with the increasing lung deposited surface area (LDSA) peaking at the size of around 100 nm for traffic sites (Lepistö et al., 2022). Due to its fine particle size and porous structure, black carbon can absorb other co-emitted compounds in ambient air, and easily penetrates human lung tissue. These toxic chemical species can be absorbed into the bloodstream through the alveolar epithelium, potentially causing cardiovascular diseases, cancers and increased premature mortality subsequently (Lepistö et al., 2022). In the most recent update to the Global Air Quality Guidelines, WHO (2021) issued a *Good Practice Statement* in relation to Black Carbon/Elemental Carbon which emphasises the need for close surveillance of Black Carbon and refers to the need for better exposure estimation and concentration prediction through dispersion modelling.

* Corresponding author.
E-mail address: r.m.harrison@bham.ac.uk (R.M. Harrison).

https://doi.org/10.1016/j.envint.2025.109265
Received 30 July 2024; Received in revised form 12 December 2024; Accepted 7 January 2025
Available online 10 January 2025

Most studies on black carbon measurement have focused on Europe, America and Asia during the last few decades, showing significant decreasing trends of black carbon concentrations, attributed to environmental control policies (Mousavi et al., 2018, Zhang et al., 2021, Jafar and Harrison, 2021, He et al., 2022). However, the source apportionment and spatio-temporal evolution of black carbon can vary depending on various anthropogenic and natural processes, geographic and meteorological conditions. Numerous studies have indicated that black carbon presents clear diurnal, weekly and seasonal patterns in the studied regions, with black carbon peaks in concentration frequently occurring at typical rush-hour times, on weekdays, and in colder seasons (Liakakou et al., 2020, Xiao et al., 2023). Although the contribution of residential heating during winter in some regions is high (Romshoo et al., 2023), traffic emissions are still considered as the main source of (black carbon) air pollution (Ciupek et al., 2021, Rovira et al., 2022). A comprehensive study which covered 50 measurement sites across Europe between 2006 and 2022, showed considerable spatio-temporal heterogeneity. The contribution of traffic emissions in most urban sites was higher than those from residential and commercial sources, but the latter were nonetheless important (Wyche et al., 2020). Savadkoohi et al. (2023) analysed equivalent black carbon (indirectly determined by light absorption techniques (Petzold et al., 2013)) data from 50 sites across Europe finding considerable heterogeneity across countries, with the highest, but declining concentrations at roadside sites, and an appreciable contribution from residential combustion.

To improve understanding of black carbon impacts in urban areas, it is necessary to better determine abundance, spatial and temporal variation. Measurements may be performed from stationary or mobile platforms; however, a comprehensive overview is hard to attain due to the limitation of sites, time, and cost. Despite low-cost black carbon sensors allowing air quality monitoring for small-area studies (Savadkoohi et al., 2023), model development combined with measured datasets retains a major role for the purpose of detailed assessment and prediction. Land-use regression is a convenient technique based on linear regression models. Road-level BC concentrations have been predicted by it, combining data from mobile monitors with GPS devices in Ghent, Belgium (Van den Hove et al., 2019). A new machine learning approach with a non-linear model has been developed for gap filling in air quality datasets in Barcelona, Spain. Black carbon concentrations can be estimated with this data-driven model (Wai et al., 2022). RLINE, based on a Gaussian formulation, is also a line-source dispersion model, which is used to simulate NO_x and BC in the San Francisco Bay Area (Patterson and Harley, 2019). Chemical transport models, such as CMAQ (Huang et al., 2023) and WRF-Chem (Rahimi et al., 2020), can be used for black carbon modelling of spatial and temporal evolution in wider regions while requiring more computational time and resources compared to the above models. ADMS-Urban, derived from the Atmospheric Dispersion Modelling System (ADMS), is an advanced program for modelling air quality from simple street scale to complex city-wide scenarios. Model results for air pollutants can be calculated and output on timescales from seconds to years, compared with monitoring data, and presented as dispersion patterns (Seaton et al., 2022). This ADMS-Urban model, sometimes combined with chemical transport models (Hood et al., 2018), has been widely used for urban air quality simulation of $PM_{2.5}$, PM_{10}, NO_x, and O_3 for the West Midlands (Zhong et al., 2021, Zhong et al., 2024), but previously not for the simulation of black carbon.

This paper presents an application of ADMS-Urban to simulate the dispersion of black carbon concentrations at street scale (10 m resolution) across the West Midlands, UK. Section 2 reports the modelling approach, and modelling cases in the study area. Section 3 presents the model evaluation and black carbon concentration maps for these modelling cases. Section 4 provides discussion on the modelling results. Section 5 gives conclusions and future research.

2. Methods

2.1. ADMS-Urban model

ADMS-Urban is the most comprehensive version of the ADMS (Atmospheric Dispersion Modelling System), which is a high-resolution air quality model based on Gaussian plume distribution (Carruthers et al., 1994). The dispersion patterns are determined by a range of meteorological inputs (e.g. wind speed, wind direction, temperature, relative humidity etc). The model considers a range of source types (e.g. road, point and grid sources), and complex urban morphology features to represent their effects on pollutant dispersion within street canyons and urban canopy layers (Hood et al., 2014). It can capture high concentration gradients near explicit road sources and generate street-scale resolution air quality maps. It is widely used all over the world in many applications, such as assessment of air quality (Hood et al., 2018, Zhang et al., 2022), investigation of air quality management options (Zhong et al., 2024), source apportionment (Blair et al., 2004), and provision of detailed street-level air quality forecasts (Stidworthy et al., 2018).

2.2. Case study

2.2.1. Study area

Fig. 1 shows the study area which covers the West Midlands region in the UK. The West Midlands has a total population of 2.9 million and a geographical area of 902 km^2. It includes 7 local authorities (among them, Birmingham is the second largest city in the UK with a high population density of 4,300/km^2). Simulations for traditional air pollutants (such as NO_2, and $PM_{2.5}$) and non-regulated ultrafine particles in the West Midlands region have been conducted using the ADMS-Urban model (Zhong et al., 2021, Zhong et al., 2023a, Zhong et al., 2024). This study extends the modelling application to the dispersion of black carbon, which is an important component of $PM_{2.5}$ and highlighted by the WHO global air quality guidelines, as outlined above (WHO, 2021). Therefore, there are a number of common model inputs (such as meteorological data, street canyon and urban canopy parameters, and spatial splitting configuration). The meteorological data as measured at the Birmingham Airport site was used in the model to drive the atmospheric dispersion (a wind rose diagram was shown in Figure S1 in Supplementary Information which indicates that the prevailing wind for the region was from the southwest). The street canyon and urban canopy parameters have been calculated based on the building geometry and road network datasets (See Zhong et al. (2021) for details). Spatial splitting configuration followed the task farming approach to optimise the run time, as adopted in Zhong et al. (2021). Other relevant model inputs specifically developed for black carbon are described as below.

2.2.2. Black carbon measurement datasets

Hourly black carbon concentration datasets over the baseline year of 2019 were obtained from the Department for Environment, Food and Rural Affairs (Defra) UK-Air website, measured using the Magee Aethalometer, model AE33 (Defra, 2019). There were only two monitoring sites in the West Midlands from the UK Black Carbon Network, Birmingham Ladywood (Lat, Lon: 52.481346, −1.918235) as an urban background site and Birmingham A4540 Roadside (Lat, Lon: 52.476145, −1.874978) as a roadside site. To compensate for insufficient black carbon measurement data, Birmingham Air Quality Supersite (BAQS) (Lat, Lon: 52.456, −1.929), an urban background site at the University of Birmingham campus provided a series of black carbon measurement data also using Magee Aethalometer, model AE33 (Bousiotis et al., 2021). The three sites as above within the West Midlands (shown in Fig. 1) were used for the model evaluation later in this study. Due to the lack of black carbon measurements to inform the regional background for the West Midlands, the Chilbolton (Lat, Lon: 51.149617, −1.438228) rural background site in the UK Black Carbon Network was used as an

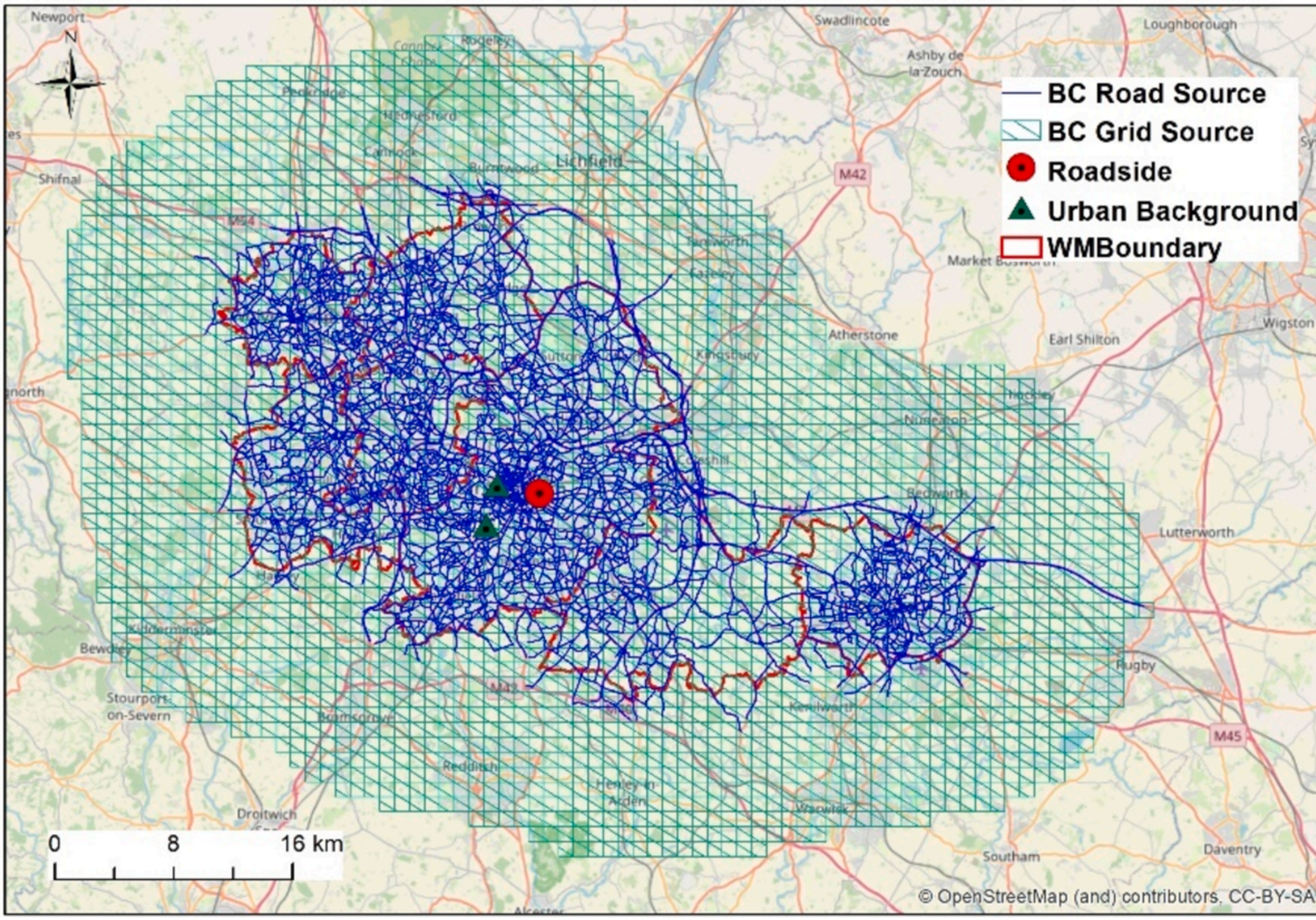

Fig. 1. West Midlands map with black carbon emission sources (Road Source and Grid Source) implemented in the model and different monitoring sites (i.e. one roadside site and two urban background sites) to be used for the model evaluation.

appropriate background site for the generation of the background input file in the ADMS-Urban model.

2.2.3. Emission inventory of black carbon

The black carbon emission inventory at 1 km × 1 km resolution for the West Midlands computational domain (Fig. 1) was obtained from the UK National Atmospheric Emissions inventory (NAEI) datasets (Tsagatakis et al., 2021). It included 11 Selected Nomenclature for Air Pollution (SNAP) sectors, as indicated in Table 1. A summary of emission sources over the West Midlands computational domain for the baseline modelling year of 2019 is given in Table 1. It indicates that SNAP08 ("Other Transport and Mobile Machinery") has the largest contribution to the black carbon emission source in the region, followed by SNAP02 (Combustion in Commercial, Industrial, Residential and Agriculture) and SNAP 07 (Road Transport including both Minor Roads and Major Roads).

Table 1
Summary of emission sources (in tonnes/year) over the West Midlands computational domain for the baseline modelling year of 2019. It is noted that there are no black carbon emissions for SNAP05 and SNAP10 from the NAEI (https://naei.energysecurity.gov.uk/emissionsapp/).

Group	Black Carbon Emissions
Major Roads	91.6
SNAP01 Combustion in Energy Production and Transformation	3.2
SNAP02 Combustion in Commercial, Industrial, Residential and Agriculture	178.1
SNAP03 Combustion in Industry	52.9
SNAP04 Production Processes	3.0
SNAP05 Extraction and Distribution of Fossil Fuels	0.0
SNAP06 Solvent Use	0.2
SNAP07 Road Transport (Minor Roads)	80.8
SNAP08 Other Transport and Mobile Machinery	217.9
SNAP09 Waste Treatment and Disposal	45.2
SNAP10 Agriculture, Forestry and Landuse Change	0.0
SNAP11 Nature (Other)	32.6

The ADMS-Urban model requires an input for the explicit road emission sources of black carbon. SNAP 07 at the 1 km × 1 km resolution from the NAEI represents the transport sector, which was then split into explicit major road sources and unresolved Minor Road gridded sources. Traffic activity and speed datasets were derived based on the traffic models from the Transport for West Midlands and Birmingham City Council (PRISM, 2019, BCC, 2018), and the bus timetable (Remix, 2019). Traffic fleet composition for the year of 2019 was obtained from the EMIT Emissions Inventory Toolkit (CERC, 2021). EMIT was used to pre-process the emission sources for black carbon with the format as required by the ADMS-Urban model. EMIT does not have direct information on the traffic emission factors for black carbon, but the emission factors for $PM_{2.5}$ calculated in Zhong et al. (2024) were used as a basis. The approach of using the ratio of black carbon to $PM_{2.5}$ was used to estimate exhaust and non-exhaust emissions of black carbon from major roads. Table 2 shows the fraction of black carbon (BC) to exhaust $PM_{2.5}$ for different vehicle categories and Euro standard as derived from the EMEP/EEA Air Pollutant Emission Inventory Guidebook (EEA, 2019), which was then implemented into EMIT for the calculation of exhaust emissions of black carbon.

Table 2
Fraction of black carbon (BC) to exhaust $PM_{2.5}$ for different vehicle categories and Euro standards (EEA, 2019).

Category	Euro standard	$BC/PM_{2.5}$ (%)
Petrol Car/LGV	Pre-Euro 1	30
	Euro 1	25
	Euro 2	25
	Euro 3	15
	Euro 4	15
	Euro 5	15
	Euro 6	15
Diesel Car/LGV	Pre-Euro 1	55
	Euro 1	70
	Euro 2	80
	Euro 3	85
	Euro 4	87
	Euro 5	20
	Euro 6	20
Diesel HDV	Pre-Euro I	50
	Euro I	65
	Euro II	65
	Euro III	70
	Euro IV	75
	Euro V	75
	Euro VI	15

Comparing with exhaust emissions, the uncertainties in non-exhaust emissions are higher (AQEG, 2019, Lugon et al., 2020) because various categories of vehicles in different driving modes at differing road locations introduce much complexity into estimation of non-exhaust emissions. An increasing number of studies now focus on non-exhaust traffic emissions due to their increasing significance as a proportion of the total emissions (Beddows and Harrison, 2021, Tomar et al., 2022). Non-exhaust emissions (as % of all traffic emissions excluding resuspension), according to estimates for respective regions (UK and EU28), present in a wide range of 5–67 % for $PM_{2.5}$ (Harrison et al., 2021). The emission factors for brake, tyre, and road wear also span wide ranges due to multiple influencing factors (Piscitello et al., 2021). To maintain consistency with previous exhaust emission factors in our case, we select the relative parameters (BC/TSP and $PM_{2.5}$/TSP ratios), both from the same guidelines (1.A.3.b.vi in (EEA, 2019)) and obtained the emission fraction of $BC/PM_{2.5}$, i.e. 36.4 % for tyre wear, 6.7 % for brake wear, and 3.9 % for road wear. These fractions of black carbon to $PM_{2.5}$ were used as the 2019 baseline model configuration. Time varying emission profiles were needed to calculate hourly emissions based on annual emissions so that the ADMS-Urban model can be run for each hour over the year. Time varying emission profiles used in this study were similar to these used in Zhong et al. (2021), with the modification of diurnal profiles for total emissions of black carbon using the deweather package in R (Carslaw and Ropkins, 2012, Grange and Carslaw, 2019) to isolate the emission contribution based on the black carbon concentration measurements at Birmingham A4540 Roadside and BAQS (Birmingham Ladywood was not used due to much lower data capture).

2.2.4. Modelling cases of traffic emission factor adjustments

As there are uncertainties for traffic emission factors of black carbon, we performed a sensitivity test of traffic emission factor adjustments. Five modeling cases were configured, respectively with an adjustment ratio of 1 (Case EF1, i.e. the 2019 baseline model configuration without adjustment), 2 (Case EF2), 3 (Case EF3), 4 (Case EF4), and 5 (Case EF5). The higher adjustment ratio cases were proposed in order to better represent the roadside based on initial assessment of the traffic emission factor case with an adjustment ratio of 3. The results of these modelling cases were evaluated and are compared in the following section.

3. Results

3.1. Model evaluation

The ADMS-Urban model was firstly configured in a "Receptor" mode for these 3 monitoring sites (Fig. 1) in the West Midlands region. Hourly modelling outputs of black carbon for the baseline year of 2019 under different modelling cases (i.e. EF1, EF2, EF3, EF4, and EF5) were generated, to be compared with the corresponding measured concentrations using the Model Evaluation Toolkit (Stidworthy et al., 2018).

Fig. 2 shows frequency scatter plots of daily averages (annual averages shown in Figure S2 in Supplementary Information) of black carbon between the modelling cases (i.e. EF1, EF2, EF3, EF4, and EF5) and measurement for both urban background and roadside sites for the year of 2019. For Case EF1, the model has a very good agreement against the measurements for the urban background sites, but with a large underestimation for the roadside site. There is an overall increase in the modelled black carbon concentrations with the increase in the adjustment ratio for the traffic emission factor for both urban background and roadside sites. Case EF3 has the best performance for the roadside site, with slight overestimation for urban background sites, indicating that an adjustment ratio of 3 for the traffic emission factor would be needed to gain an appropriate fit for the roadside site. An adjustment ratio of 5 (Case EF 5) gives larger overestimation for both urban background and roadside sites. Consideration was given to whether local effects were leading to anomalously high concentrations at the roadside site, but this seems unlikely as it is an open site, not subject to street canyon effects upon dispersion (https://uk-air.defra.gov.uk/networks/site-info?site_id=BIRR), and model simulations of NOx at this site worked well (Zhong et al., 2024).

Table 3 shows the model evaluation statistics calculated from the hourly modelled and measured concentrations of black carbon for all five modelling cases (i.e. EF1, EF2, EF3, EF4, and EF5) for the year of 2019. Observed and modelled annual concentrations (denoted by Obs and Mod, respectively in Table 3) were also reflected in the scatter plots in Fig. 2. Modelled annual concentrations in Table 3 further demonstrated a nearly linear relationship with the adjustment ratio of the traffic emission factor for these three sites within the West Midlands. NMSE (Normalised Mean Square Error measuring the mean difference between the model and measurement) is relatively smaller for Cases EF3 and EF4 at Birmingham A4540 Roadside and Birmingham Ladywood sites, and for Cases EF2 and EF3 at BAQS. R (correlation coefficient) is in the similar range for all modelling cases, i.e. within (0.46, 0.48) for roadside site and (0.57, 0.61) for urban background sites. Fac2 (fraction of modelled data within a factor of 2 of observations) has the largest value for Case EF3 at roadside site, and for Case EF1 at urban background sites. Fb (fraction bias) has the smallest magnitude for Case EF3 at roadside site, and for Case EF1 at urban background sites. Overall, Case EF3 works best for the roadside site (with a slight overestimation of 3 % in annual concentration) in this study, while Case EF1 works best for urban background sites (although with a slight overestimation of 3–5 % in annual concentration).

Fig. 3 shows time variation analysis between modelled (for Cases EF1, EF2, EF3, EF4, and EF5) and measured black carbon concentrations at the Birmingham A4540 roadside for the year of 2019. With an increase of the adjustment ratio for the traffic emission factor, time variation profiles (i.e. hour of the day, day of the week and month of the year) of the modelled black carbon concentration shift upward (i.e. an increase). Case EF1 significantly underestimated these measured time variation profiles, while Case EF2 slightly underestimated these profiles. Case EF3 has the best performance in capturing these measured time variation profiles, as seen clearly in Fig. 3. Further increasing the adjustment ratio for the traffic emission factor as in Cases EF4 and EF5, the model would then give a further overestimation. However, for the time variation analysis at urban background sites (Fig. 4 for BAQS and Figure S3 in Supplementary Information for Birmingham Ladywood),

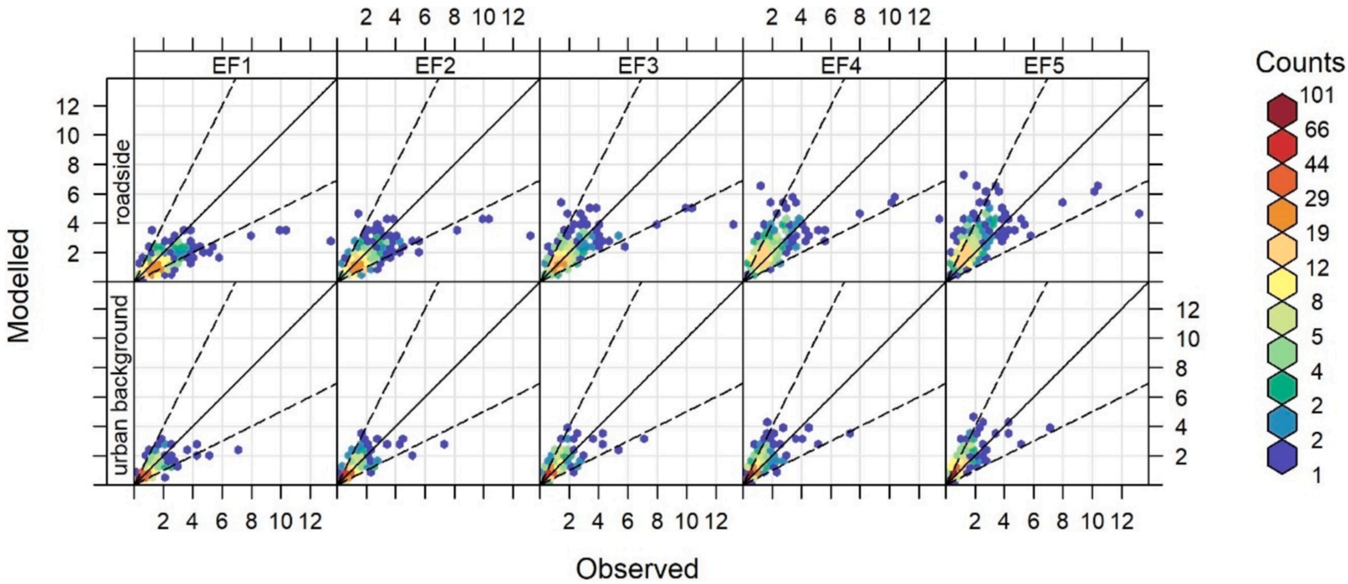

Fig. 2. Frequency scatter plots of daily averages of black carbon (in μg m^{-3}) between the modelling cases (i.e. EF1, EF2, EF3, EF4, and EF5) and measurement for both urban background and roadside sites for the year of 2019.

Table 3
Model evaluation statistics calculated from the hourly modelled and measured concentrations of black carbon for all five modelling cases (i.e. EF1, EF2, EF3, EF4, and EF5) for the year of 2019. Obs: observed annual concentration; Mod: modelled annual concentration; NMSE: normalised mean square error; R: correlation coefficient; Fac2: fraction of modelled data within a factor of 2 of observations; Fb: fraction bias.

Station	Type	Case EF	Obs (μg m^{-3})	Mod (μg m^{-3})	NMSE	R	Fac2	Fb
Birmingham A4540 Roadside	roadside	EF1	1.80	1.23	1.27	0.48	0.57	−0.37
		EF2	1.80	1.54	0.94	0.48	0.65	−0.15
		EF3	1.80	1.86	0.82	0.47	0.68	0.03
		EF4	1.80	2.17	0.81	0.47	0.67	0.19
		EF5	1.80	2.48	0.87	0.46	0.64	0.32
Birmingham Ladywood	urban background	EF1	1.37	1.33	1.06	0.57	0.73	−0.03
		EF2	1.37	1.51	0.94	0.58	0.71	0.10
		EF3	1.37	1.68	0.89	0.58	0.66	0.21
		EF4	1.37	1.86	0.89	0.59	0.62	0.30
		EF5	1.37	2.04	0.93	0.59	0.59	0.39
BAQS	urban background	EF1	0.78	0.74	0.83	0.61	0.73	−0.05
		EF2	0.78	0.83	0.76	0.61	0.73	0.07
		EF3	0.78	0.93	0.75	0.61	0.72	0.17
		EF4	0.78	1.02	0.79	0.61	0.69	0.26
		EF5	0.78	1.11	0.85	0.60	0.66	0.35

Case EF1 has the best model performance. With the increase in the the adjustment ratio, the modelled time variation profiles tend to shift upwards.

3.2. Black carbon concentration maps

In order to generate black carbon concentration maps, the ADMS-Urban model was then configured in a "Contour" mode to include dense output points over the West Midlands region (Same configuration as that in Zhong et al. (2021)). The Linux version of the ADMS-Urban model was run in parallel using the task farming approach (Zhong et al., 2021) for the spatial splitting of the computational domain. An array job with 540 cores for each subdomain was submitted to the University of Birmingham's BlueBEAR HPC. It took about 18 h' elapse time to complete a typical whole year simulation. CombineCOF and AddInterpIGP utilities were applied to combine and interpolate output files from each subdomain in Linux. The "Process comprehensive output" utility built in the ADMS-Urban model was used to derive the annual averages for all the output points over the West Midlands region, which was imported into Surfer (GoldenSoftware, 2023) to generate contour maps. These contour maps of black carbon were visualised in ArcGIS (ESRI, 2023), and are reported below.

Fig. 5a shows annual concentration maps of black carbon for the year of 2019 at 10 m × 10 m resolution for Case EF3 (with best performance for roads). There are clearly visible spatial patterns induced by the dispersion of explicit road emission sources over the West Midlands. Higher annual BC concentrations were found near the highways or major roads in city centre areas, especially on the A41 road running transversely through the West Midlands area, A38(M) across the centre of Birmingham and M5 across the centre of Oldbury. The highest concentrations of black carbon near roads can reach 8.5 μg m^{-3} for Case EF3 with an adjustment ratio of 3 for the traffic emission factor. Relatively lower BC concentrations are mainly distributed in rural areas, and in areas away from major roads. With the increase of the adjustment ratio of the traffic emission factor, black carbon concentrations increase spatially across the whole West Midlands (as indicated in Figure S4 Supplementary Information). Fig. 5b further shows predicted black carbon concentrations at local authority level (Boundary lines shown in Figure S5 in Supplementary Information) against the adjustment ratio of the traffic emission factor. There are linear relationships between black

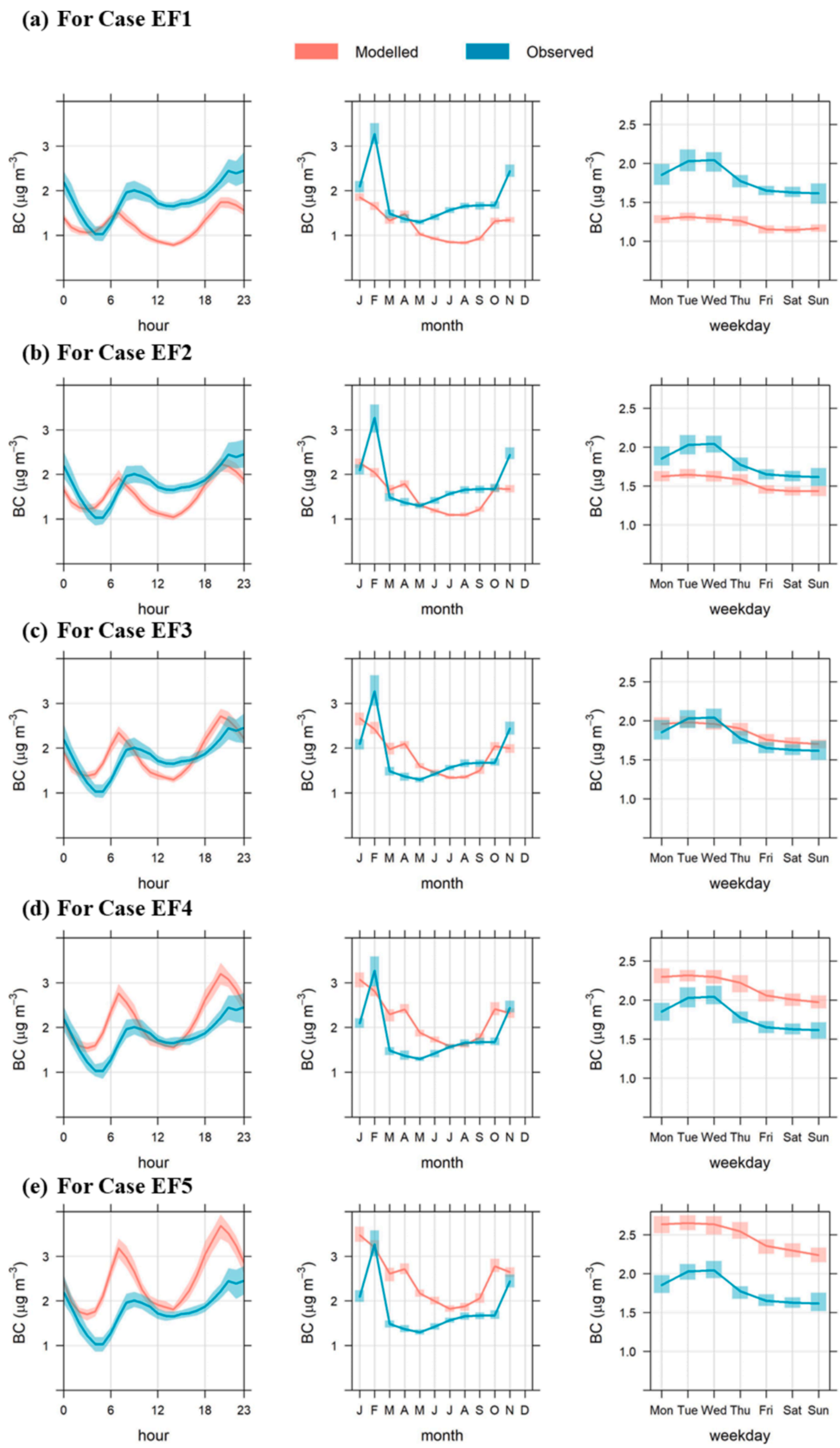

Fig. 3. Time variation analysis between modelled (for Cases EF1, EF2, EF3, EF4, and EF5) and measured black carbon (BC in µg m^{-3}) concentrations at Birmingham A4540 roadside for the year of 2019.

carbon concentrations and the adjustment ratio for all seven local authorities within the West Midlands. Sandwell has the highest level of black carbon, followed by Birmingham, while Solihull has the lowest level of black carbon.

Fig. 6a-e presents annual concentration maps of black carbon for the year of 2019 at the electoral ward level (averaged over the 10 m × 10 m resolution concentration maps over the ward) for all five modelling cases. The ward level black carbon concentration datasets could be useful for further health-related assessment, such as the ward level Air Quality Lifecourse Assessment Tool (AQ-LAT Hall et al. (2024)), and

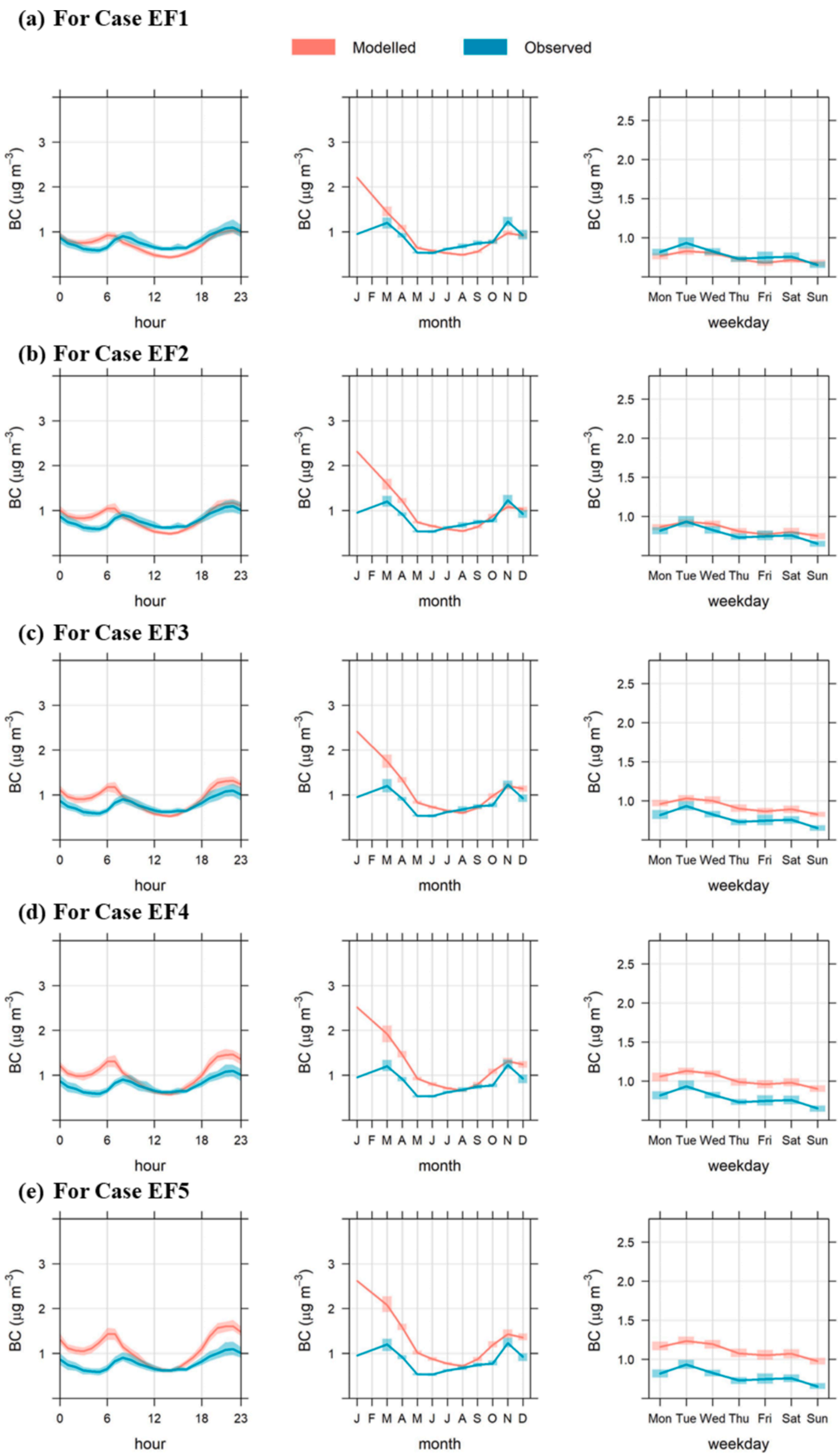

Fig. 4. Time variation analysis between modelled (for Cases EF1, EF2, EF3, EF4, and EF5) and measured black carbon (BC in μg m^{-3}) concentrations at BAQS (Urban background site) for the year of 2019.

(a) For Case EF3 (b) BC at LA level for all cases

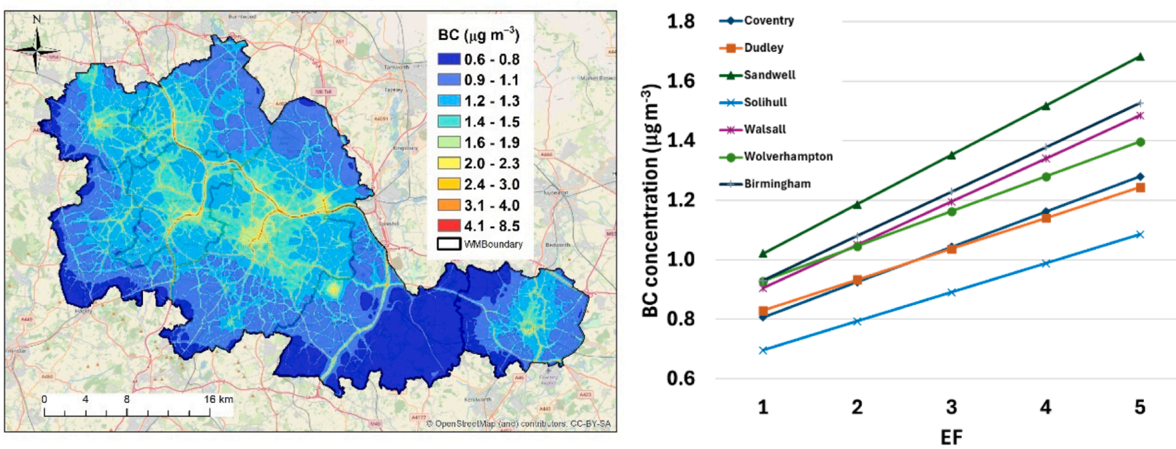

Fig. 5. Annual concentration maps of black carbon (BC in μg m^{-3}) for the year of 2019 at 10 m × 10 m resolution for (a) Case EF3 (with best performance for roads), and (b) BC at local authority level (LA) for all cases. Note, Annual concentration maps for other EF cases are presented in the Supplementary Information.

(a) For Case EF3 (b) BC at ward level for all cases

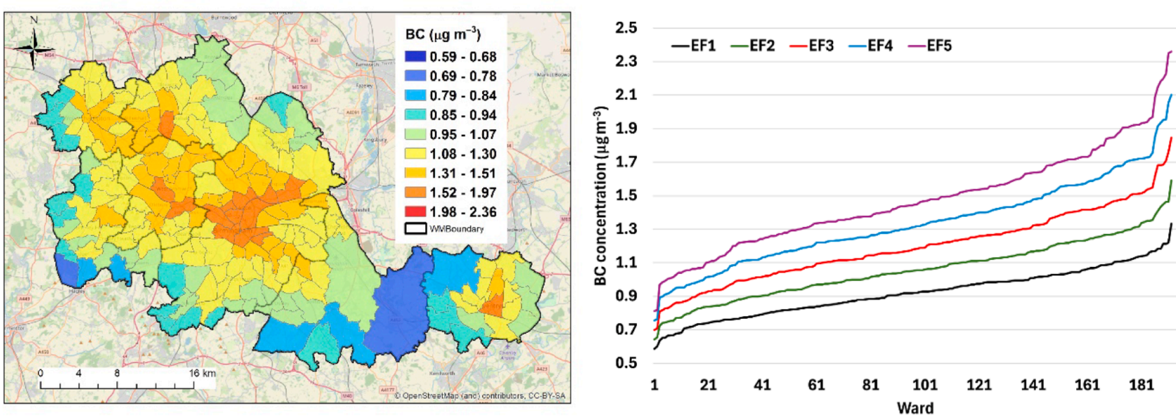

Fig. 6. Annual concentration maps of black carbon (BC in μg m^{-3}) at the ward level for (a) Case EF3, (b) BC at ward level (ranking BC from the smallest to the largest) for all cases. Note, Annual concentration maps for other EF cases are presented in the Supplementary Information.

which have previously only been performed for NO_2 and $PM_{2.5}$. AQ-LAT is a ward-level tool to estimate the impacts of pollutant exposure on health and economic outcomes (e.g. morbidity, mortality, and associated healthcare costs), which can be used to assess localised policy decisions (Hall et al., 2024). Relatively higher annual BC concentrations occur in wards in city centre areas. The range of black carbon at the ward level is smaller and narrower, compared with the 10 m × 10 m resolution concentration maps. This is due to the spatial averaging adopted, which does not show the highest concentrations near explicit road sources. Higher ward-level concentrations of black carbon are also found for cases with larger adjustment ratios of the traffic emission factor (as indicated in Figure S6 Supplementary Information). Fig. 6b further shows black carbon concentrations at ward level (ranking from the smallest to the largest) for all five modelling cases. Similarly, nearly linear relationships between black carbon concentrations and the adjustment ratio for all wards were observed. The increment of black carbon concentration is generally lower for the wards with smaller values, and higher for the wards with larger values.

4. Discussion

The ADMS-Urban modelling configuration for prediction of black carbon concentrations has been evaluated against (a limited number of) monitoring sites. Scatter plots of annual averages of black carbon demonstrated that there is a very good agreement between Case EF1 with an unadjusted traffic emission factor and measurements for the urban background sites. It suggests that adjustment for the traffic emission factor would not be needed if the research focus is solely on urban background sites, such as the application in coarse resolution regional air quality modelling (without explicitly resolving localised traffic emissions, e.g. the WRF-CMAQ model of Mazzeo et al. (2022)). An adjustment ratio of 3 for the traffic emission factor (Case EF3) is needed to better represent the roadside site (also indicated in Table 3). Road traffic emission factors are normally with large uncertainties and real-world adjustments are widely adopted in modelling practise, e.g. Hood et al. (2018). There may be the possibility of some near-road missing emission sources, such as from idling vehicles and from non-road mobile machinery on construction sites. Future source apportionment studies for both urban background and roadside sites could provide useful insights in the contributions of black carbon concentrations from traffic, wood burning and other sources. It is challenging to obtain representative or accurate traffic emission factors for black carbon from published literature. Various studies provide a large range of traffic emission factors. Some studies have suggested an increasing trend of traffic emission factors for non-exhaust emissions, such as tyre-wear, brake-wear and road surface-wear emissions (Beddows and Harrison, 2021, Wen et al., 2019, Lugon et al., 2020, Harrison et al., 2021). There are various factors which may affect the black carbon emissions, such as road surface conditions, vehicle types, and driving behaviour (Ghaffarpasand and Pope, 2024). Vehicle electrification under Net Zero pathways would reduce exhaust emissions from tail pipes, but non-exhaust emissions remain (Zhong et al., 2023b). The time variation analysis also indicates overall good fits for the modelled and observed black carbon concentrations for the roadside site for Case EF3. Higher black carbon concentrations occur at traffic rush hour times and in colder months. This is not surprising as during rush hours there are more vehicles traveling on the roads and releasing more pollutants. In colder months, the lower mixed layer height and stable atmospheric conditions make the dispersion worse, which leads to the accumulation of black carbon. The need for an emissions adjustment factor as large as 3 is quite surprising. It may reflect errors in the BC/$PM_{2.5}$ ratios used, or more likely the influence of defective diesel particle filters and vehicle tampering, involving removal of emissions control devices, upon overall fleet emissions. In this study, the uncertainty of BC emissions in the road transport sector was investigated via adjusting traffic emission factors, which is the single most simple and practical adjustment to emissions in order to bring the model into reasonable agreement with the observations at the roadside site. However, there may be uncertainties relating to other sectors, such as residential combustion, industry and non-road transport, which may also be influential. The BC stations located at Birmingham city centre areas may be less influenced by emission from other sectors compared with the road transport sector while the BAQS station located at the University of Birmingham in a sub-urban area may be more influenced by other sectors. In this study, there are only 2 urban background sites and 1 roadside site available for the model evaluation. More measurements for unregulated black carbon are needed as highlighted by the Global Air Quality Guidelines, WHO (2021). The use of different mass absorption cross-section coefficients for BC in emission and ambient concentration measurements would also have an effect upon the data (Ciupek et al., 2021). Filter-based absorption photometers (such as the Aethalometer) measure the attenuation of light passing through particulate matter collected on a filter and estimate black carbon mass concentrations from the light attenuation using mass absorption cross-section coefficients (Savadkoohi et al., 2023, Drinovec et al., 2015). Mass absorption cross-section coefficients are wavelength dependent and can vary with sample composition, particle size and shape, which leads to uncertainties in estimating black carbon mass concentrations (Petzold et al., 2013).

In order to generate high resolution spatial distributions for black carbon concentrations over the whole West Midlands, the ADMS-Urban model needs to be run in the "Contour" mode (Zhong et al., 2021, Zhong et al., 2024). Black carbon maps at 10 m × 10 m resolution can capture the high concentration gradient near road sources, especially for motorways and city centre areas with denser traffic volume. Street-canyon geometries in the urban area could be another factor which prevents the dispersion of black carbon in the street canyon environments (Hood et al., 2014). With the increase of the adjustment ratio of the traffic emission factor, there is an increase in black carbon concentration spatially across the whole West Midlands. Traffic emission factors of black carbon should be considered as an important element in the modelling. This study demonstrated a linear relationship between black carbon concentration (considered as a passive scalar in this study) and the traffic emission factor adjustment ratio, which suggests that future relevant traffic-related scenarios could be simply calculated without running sophisticated and time-consuming dispersion modelling. The 10 m × 10 m resolution maps can be spatially aggregated into health-related ward level and local authority level. The ward level concentration maps could be linked with health assessment in future, such as extending the ward level AQ-LAT health tool (Hall et al., 2024) to also including black carbon. Lepistö et al. (2022) reported that ambient black carbon would correlate with lung-depositing surface area of particles, which may show an association with health effects. This work can assist research on the relationship between exposure to black carbon and health, especially in city areas.

5. Conclusions

This study developed a dispersion model to simulate the dispersion of black carbon concentrations over the West Midlands, UK. The sensitivity test of traffic emission factor adjustments was conducted and evaluated against the measurements at all three available monitoring sites (2 urban background sites and 1 roadside site) within the region. The model overall has good performance. The modelling case with an unadjusted traffic emission factor can well capture black carbon annual concentrations at urban background sites. An adjustment ratio of 3 for the traffic emission factor is needed to better represent the roadside site (although with a slight overestimation of 3 % in annual concentration) in this study. There are linear relationships between black carbon concentrations and the adjustment ratio for the traffic emission factor. Black carbon concentration maps have been generated at 10 m × 10 m resolution, which were then aggregated into health-related ward level and local authority level.

Future research could be 1) to explore the effects of traffic management policies (e.g. clean air zone, reducing traffic speed limit), 2) to intercompare other dispersion models and conduct sensitivity tests of traffic emission factor adjustments, 3) to further develop the AQ-LAT health tool for black carbon and conduct health risk and inequality assessments, and 4) to conduct the sensitivity test of other significant emission sectors such as residential heating, industrial activities, and non-road mobile sources.

CRediT authorship contribution statement

Jian Zhong: Writing – original draft, Visualization, Software, Methodology, Formal analysis, Conceptualization. **Yinghua Li:** Writing – original draft, Visualization, Software, Methodology. **William James Bloss:** Writing – review & editing, Supervision, Funding acquisition. **Roy M. Harrison:** Writing – review & editing, Writing – original draft, Supervision, Funding acquisition, Conceptualization.

Funding

This work has been supported by the European Union's Horizon 2020 research and innovation programme under grant agreement No 101,036,245 (RI-URBANS project). JZ acknowledges the funding from the UK's NERC WM-Air project (grant number NE/S003487/1), Wellcome Trust WM-Net Zero project (Ref: 227150/Z/23/Z), EPSRC CLEETS project (grant number EP/Y026233/1). YL thanks to China Scholarship Council for the financial support of visiting the University of Birmingham (Ref: 202108220137).

Declaration of competing interest

The authors declare that they have no known competing financial interests or personal relationships that could have appeared to influence the work reported in this paper.

Acknowledgments

The authors acknowledge the University of Birmingham's BlueBEAR HPC service (http://www.birmingham.ac.uk/bear) for providing the computational resource and thank Cambridge Environmental Research

Consultants for provision of the ADMS-Urban model and licence. The authors appreciate Transport for West Midlands and Birmingham City Council for provision of traffic data, previous modelling and reports. The authors also appreciate Siqi Hou for the provision of Birmingham Air Quality Supersite measurement data for black carbon.

Appendix A. Supplementary data

Supplementary data to this article can be found online at https://doi.org/10.1016/j.envint.2025.109265.

Data availability

AURN data are available via Defra website, https://uk-air.defra.gov.uk/networks/network-info?view=aurn. The NAEI emission datasets for black carbon are available via http://naei.beis.gov.uk/data. MIDAS met data are available via http://data.ceda.ac.uk/badc. EMEP time-variation data are available via https://www.emep.int/. The building data are available via https://digimap.edina.ac.uk. Modelled black carbon annual concentration maps are openly available from the UBIRA eData repository at https://doi.org/10.25500/edata.bham.00001141.

References

AQEG 2019. Non-Exhaust Emissions from Road Traffic. Air Quality Expert Group. https:// uk-air.defra.gov.uk/library/reports?report_id=992.

BCC. 2018. *Birmingham Clean Air Zone Feasibility Study* [Online]. Available: https://www.birmingham.gov.uk/download/downloads/id/11353/aq3_-_birmingham_caz_fbc_report-_air_quality_v3_4-12-18.pdf+&cd=1&hl=zh-CN&ct=clnk&gl=uk [Accessed 1 October 2019].

Beddows, D.C.S., Harrison, R.M., 2021. PM10 and PM2.5 emission factors for non-exhaust particles from road vehicles: Dependence upon vehicle mass and implications for battery electric vehicles. *Atmos. Environ.* 244, 117886.

Blair, J., Johnson, K. & Carruthers, D. J. 2004. Source Apportionment for London using ADMS-Urban, https://naei.beis.gov.uk/reports/reports?report_id=234.

Bond, T.C., Doherty, S.J., Fahey, D.W., Forster, P.M., Berntsen, T., Deangelo, B.J., Flanner, M.G., Ghan, S., Kärcher, B., Koch, D., Kinne, S., Kondo, Y., Quinn, P.K., Sarofim, M.C., Schultz, M.G., Schulz, M., Venkataraman, C., Zhang, H., Zhang, S., Bellouin, N., Guttikunda, S.K., Hopke, P.K., Jacobson, M.Z., Kaiser, J.W., Klimont, Z., Lohmann, U., Schwarz, J.P., Shindell, D., Storelvmo, T., Warren, S.G., Zender, C.S., 2013. Bounding the role of black carbon in the climate system: a scientific assessment. *J. Geophys. Res. Atmos.* 118, 5380–5552.

Bousiotis, D., Singh, A., Haugen, M., Beddows, D.C.S., Diez, S., Murphy, K.L., Edwards, P. M., Boies, A., Harrison, R.M., Pope, F.D., 2021. Assessing the sources of particles at an urban background site using both regulatory instruments and low-cost sensors – a comparative study. *Atmos. Meas. Tech.* 14, 4139–4155.

Carruthers, D.J., Holroyd, R.J., Hunt, J.C.R., Weng, W.S., Robins, A.G., Apsley, D.D., Thompson, D.J., Smith, F.B., 1994. UK-ADMS: A new approach to modelling dispersion in the earth's atmospheric boundary layer. *J. Wind Eng. Ind. Aerodyn.* 52, 139–153.

Carslaw, D.C., Ropkins, K., 2012. openair — An R package for air quality data analysis. *Environ. Model. Softw.* 27–28, 52–61.

CERC. 2021. *EMIT Atmospheric Emissions Inventory Toolkit User Guide* [Online]. Available: http://www.cerc.co.uk/environmental-software/assets/data/doc_userguides/CERC_EMIT3.4_UserGuide.pdf [Accessed 26 March 2021].

Ciupek, K., Quincey, P.G., Green, D.C., Butterfield, D.M., Fuller, G.W., 2021. *Challenges and policy implications of long-term changes in mass absorption cross-section derived from equivalent black carbon and elemental carbon measurements in London and south-east England in 2014-2019. Environ. Sci. Processes Impacts*.

DEFRA. 2019. *Automatic Urban and Rural Network (AURN)* [Online]. Available: https://uk-air.defra.gov.uk/networks/network-info?view=aurn [Accessed 18 June 2019].

Drinovec, L., Močnik, G., Zotter, P., Prévôt, A.S.H., Ruckstuhl, C., Coz, E., Rupakheti, M., Sciare, J., Müller, T., Wiedensohler, A., Hansen, A.D.A., 2015. The "dual-spot" Aethalometer: an improved measurement of aerosol black carbon with real-time loading compensation. *Atmos. Meas. Tech.* 8, 1965–1979.

Eckhardt, S., Pisso, I., Evangeliou, N., Zwaaftink, C.D.G., Plach, A., McConnell, J.R., Sigl, M., Ruppel, M.M., Zdanowicz, C., Lim, S., Chellman, N.J., Opel, T., Meyer, H., Steffensen, J.P., Schwikowski, M., Stohl, A., 2023. Revised historical Northern Hemisphere black carbon emissions based on inverse modeling of ice core records. *NatureCommunications* 14.

EEA 2019. EMEP/EEA Air Pollutant Emission Inventory Guidebook. Technical Guidance to Prepare National Emission Inventories. EEA Report No 13/2019. https://www.eea.europa.eu/publications/emep-eea-guidebook-2019.

ESRI. 2023. *ArcGIS Desktop A complete suite for desktop GIS* [Online]. Available: https://www.esri.com/en-us/arcgis/products/arcgis-desktop/overview [Accessed 15 September 2023].

Ghaffarpasand, O., Pope, F.D., 2024. Telematics data for geospatial and temporal mapping of urban mobility: New insights into travel characteristics and vehicle specific power. *J. Transp. Geogr.* 115, 103815.

Goldensoftware. 2023. *Surfer Explore the Depths of Your Data* [Online]. Available: https://www.goldensoftware.com/products/surfer/ [Accessed 15 September 2023].

Grange, S.K., Carslaw, D.C., 2019. Using meteorological normalisation to detect interventions in air quality time series. *Sci. Total Environ.* 653, 578–588.

Hall, J., Zhong, J., Jowett, S., Mazzeo, A., Thomas, G.N., Bryson, J.R., Dewar, S., Inglis, N., Wolstencroft, M., Muller, C., Bloss, W., Harrison, R., Bartington, S., 2024. Regional impact assessment of air quality improvement: The air quality lifecourse assessment tool (AQ-LAT) for the West Midlands combined authority (WMCA) area. *Environ. Pollut.*

Hansel, N.N., Romero, K., Pollard, S.L., Bose, S., Psoter, K.J., Underhill, L.J., Johnson, C., Williams, D.A.L., Curriero, F.C., Breysse, P.N., Koehler, K.A., Checkley, W., 2018. Ambient air pollution and variation in multiple domains of asthma morbidity among peruvian children. *Ann. Am. Thorac. Soc.* 16, 348–355.

Harrison, R.M., Allan, J.D., Carruthers, D., Heal, M.R., Lewis, A.C., Marner, B.B., Murrells, T.P., Williams, A.M., 2021. Non-exhaust vehicle emissions of particulate matter and VOC from road traffic: A review. *Atmos. Environ.* 262, 118592.

He, C., Ye, Z., Wu, Q., Liu, L., Zhao, Y., Ni, J., Li, B., Niu, X., Jin, J., 2022. Black carbon pollution in china from 2001 to 2019: Patterns, trends, and drivers. *SSRN Electron. J.*.

Healy, R.M., Wang, J.M., Sofowote, U.M., Su, Y., Debosz, J., Noble, M., Munoz, A., Jeong, C.-H., Hilker, N., Evans, G.J., Doerksen, G., 2019. Black carbon in the Lower Fraser Valley, British Columbia: Impact of 2017 wildfires on local air quality and aerosol optical properties. *Atmos. Environ.*

HOOD, C., CARRUTHERS, D., SEATON, M., STOCKER, J. & JOHNSON, K. 2014. Urban canopy flow field and advanced street canyon modelling in ADMS-Urban. *In 16th International Conference on Harmonisation, Varna, Bulgaria, 8-11 September 2014; pp. 8-11*.

Hood, C., Mackenzie, I., Stocker, J., Johnson, K., Carruthers, D., Vieno, M., Doherty, R., 2018. Air quality simulations for London using a coupled regional-to-local modelling system. *Atmos. Chem. Phys.* 18, 11221–11245.

Huang, Y., Lu, X., Li, Z., Fung, J. & Wong, D. 2023. Direct radiative effects of black carbon and brown carbon from Southeast Asia biomass burning with the WRF-CMAQ two-way coupled model. *EGU General Assembly Conference Abstracts.* Vienna, Austria.

Jafar, H.A., Harrison, R.M., 2021. Spatial and temporal trends in carbonaceous aerosols in the United Kingdom. *Atmos. Pollut. Res.* 12, 295–305.

Janssen, N.A.H., Hoek, G., Simic-Lawson, M., Fischer, P., Bree, L.V., Brink, H.T., Keuken, M., Atkinson, R.W., Anderson, H.R., Brunekreef, B., Cassee, F.R., 2011. Black carbon as an additional indicator of the adverse health effects of airborne particles compared with PM_{10} and $PM_{2.5}$. *Environ. Health Perspect.* 119, 1691–1699.

Johnson, B.T., Shine, K.P., Forster, P.M., 2004. The semi-direct aerosol effect: Impact of absorbing aerosols on marine stratocumulus. *Q. J. R. Meteorolog. Soc.* 130, 1407–1422.

Jung, K.H., Lovinsky-Desir, S., Yan, B., Torrone, D.Z., Lawrence, J., Jezioro, J.R., Perzanowski, M.S., Perera, F.P., Chillrud, S.N., Miller, R.L., 2017. Effect of personal exposure to black carbon on changes in allergic asthma gene methylation measured 5 days later in urban children: importance of allergic sensitization. *Clinical Epigenetics* 9.

Kang, S., Zhang, Y., Qian, Y., Wang, H., 2020. A review of black carbon in snow and ice and its impact on the cryosphere. *Earth Sci. Rev.* 210, 103346.

Koch, D., Schulz, M., Kinne, S., McNaughton, C., Spackman, J.R., Balkanski, Y., Bauer, S., Berntsen, T., Bond, T.C., Boucher, O., Chin, M., Clarke, A., de Luca, N., Dentener, F., Diehl, T., Dubovik, O., Easter, R., Fahey, D.W., Feichter, J., Fillmore, D., Freitag, S., Ghan, S., Ginoux, P., Gong, S., Horowitz, L., Iversen, T., Kirkevåg, A., Klimont, Z., Kondo, Y., Krol, M., Liu, X., Miller, R., Montanaro, V., Moteki, N., Myhre, G., Penner, J.E., Perlwitz, J., Pitari, G., Reddy, S., Sahu, L., Sakamoto, H., Schuster, G., Schwarz, J.P., Seland, O., Stier, P., Takegawa, N., Takemura, T., Textor, C., van Aardenne, J.A., Zhao, Y., 2009. Evaluation of black carbon estimations in global aerosol models. *Atmos. Chem. Phys.* 9, 9001–9026.

Lepistö, T., Kuuluvainen, H., Lintusaari, H., Kuittinen, N., Salo, L., Helin, A., Niemi, J.V., Manninen, H.E., Timonen, H., Jalava, P., Saarikoski, S., Rönkkö, T., 2022. Connection between lung deposited surface area (LDSA) and black carbon (BC) concentrations in road traffic and harbour environments. *Atmos. Environ.* 272, 118931.

Li, W., Liu, X., Duan, F., Qu, Y., An, J., 2022. A one-year study on black carbon in urban Beijing: Concentrations, sources and implications on visibility. *Atmos. Pollut. Res.*

Liakakou, E., Stavroulas, I., Kaskaoutis, D.G., Grivas, G., Paraskevopoulou, D., Dumka, U. C., Tsagkaraki, M., Bougiatioti, A., Oikonomou, K., Sciare, J., Gerasopoulos, E., Mihalopoulos, N., 2020. Long-term variability, source apportionment and spectral properties of black carbon at an urban background site in Athens, Greece. *Atmos. Environ.* 222, 117137.

Liu, X., Penner, J.E., Wang, M., 2009. Influence of anthropogenic sulfate and black carbon on upper tropospheric clouds in the NCAR CAM3 model coupled to the IMPACT global aerosol model. *J. Geophys. Res. Atmospheres* 114.

Lugon, L., Vigneron, J., Debert, C., Chrétien, O. & Sartelet, K. Black carbon modelling in urban areas: investigating the influence of resuspension and non-exhaust emissions in streets using the Street-in-Grid (SinG) model. 2020.

Mazzeo, A., Zhong, J., Hood, C., Smith, S., Stocker, J., Cai, X., Bloss, W.J., 2022. Modelling the impact of national vs. local emission reduction on PM2.5 in the west midlands, UK using WRF-CMAQ. *Atmos.* 13, 377.

Mousavi, A., Sowlat, M.H., Hasheminassab, S., Polidori, A., Sioutas, C., 2018. Spatio-temporal trends and source apportionment of fossil fuel and biomass burning black carbon (BC) in the Los Angeles Basin. *Sci. Total Environ.* 640–641, 1231–1240.

Oshima, N., Koike, M., Zhang, Y., Kondo, Y., Moteki, N., Takegawa, N., Miyazaki, Y., 2009. Aging of black carbon in outflow from anthropogenic sources using a mixing state resolved model: Model development and evaluation. *J. Geophys. Res.-Atmos.* 114.

Patterson, R.F., Harley, R.A., 2019. Evaluating near-roadway concentrations of diesel-related air pollution using RLINE. *Atmos. Environ.*
Petzold, A., Ogren, J.A., Fiebig, M., Laj, P., Li, S.M., Baltensperger, U., Holzer-Popp, T., Kinne, S., Pappalardo, G., Sugimoto, N., Wehrli, C., Wiedensohler, A., Zhang, X.Y., 2013. Recommendations for reporting "black carbon" measurements. *Atmos. Chem. Phys.* 13, 8365–8379.
Piscitello, A., Bianco, C., Casasso, A., Sethi, R., 2021. Non-exhaust traffic emissions: Sources, characterization, and mitigation measures. *Sci. Total Environ.* 766, 144440.
PRISM 2019. Available: https://corporate.tfwm.org.uk/strategy/data-insight/transport-modelling/about-prism/ [accessed on 22 July 2019].
Rahimi, S., Liu, X., Zhao, C., Lu, Z., Lebo, Z.J., 2020. Examining the atmospheric radiative and snow-darkening effects of black carbon and dust across the Rocky Mountains of the United States using WRF-Chem. *Atmos. Chem. Phys.* 20, 10911–10935.
Ramanathan, V., Carmichael, G., 2008. Global and regional climate changes due to black carbon. *Nat. Geosci.* 1, 221–227.
REMIX 2019. Available: https://www.remix.com/.
Réveillet, M., Dumont, M., Gascoin, S., Lafaysse, M., Nabat, P., Ribes, A., Nheili, R., Tuzet, F., Ménégoz, M., Morin, S., Picard, G., Ginoux, P.A., 2021. Black carbon and dust alter the response of mountain snow cover under climate change. *Nat. Commun.* 13.
Romshoo, B., Bhat, M.A., Habib, G., 2023. Black carbon in contrasting environments in India: Temporal variability, source apportionment and radiative forcing. *Atmos. Environ.*
Rovira, J., Paredes-Ahumada, J.A., Barceló-Ordinas, J.M., Vidal, J.G., Reche, C., Sola, Y., Fung, P., Petäjä, T., Hussein, T., Viana, M., 2022. Non-linear models for black carbon exposure modelling using air pollution datasets. *Environ. Res.*
Savadkoohi, M., Pandolfi, M., Reche, C., Niemi, J.V., Mooibroek, D., Titos, G., Green, D. C., Tremper, A.H., Hueglin, C., Liakakou, E., Mihalopoulos, N., Stavroulas, I., Artíñano, B., Coz, E., Alados-Arboledas, L., Beddows, D.C.S., Riffault, V., de Brito, J. F., Bastian, S., Baudic, A., Colombi, C., Costabile, F., Chazeau, B., Marchand, N., Luis Gómez-Amo, J., Estellés, V., Matos, V., Van der gaag, E., Gille, G., Luoma, K., Manninen, H.E., Norman, M., Silvergren, S., Petit, J.-E., Putaud, J.-P., Rattigan, O.V., Timonen, H.J., Tuch, T., Merkel, M., Weinhold, K., Vratolis, S., Vasilescu, J., Favez, O., Harrison, R.M., Laj, P., Wiedensohler, A., Hopke, P.K., Petäjä, T., Alastuey, A., Querol, X., 2023. The variability of mass concentrations and source apportionment analysis of equivalent black carbon across urban Europe. *Environ. Int.* 178, 108081.
Seaton, M.D., O'Neill, J., Bien, B., Hood, C., Jackson, M., Jackson, R., Johnson, K., Oades, M., Stidworthy, A., Stocker, J., Carruthers, D., 2022. A multi-model air quality system for health research: road model development and evaluation. *Environ. Model. Softw.* 155, 105455.
Stidworthy, A., Jackson, M., Johnson, K., Carruthers, D., Stocker, J., 2018. Evaluation of local and regional air quality forecasts for London. *Int. J. Environ. Pollut.* 64, 178–191.
Tomar, G., Nagpure, A.S., Kumar, V., Jain, Y., 2022. High resolution vehicular exhaust and non-exhaust emission analysis of urban-rural district of India. *Sci. Total Environ.* 805, 150255.
Tsagatakis, I., Richardson, J., Evangelides, C., Pizzolato, M., Pearson, B., Passant, N., Pommier, M. & Otto, A. 2021. UK Spatial Emissions Methodology: A report of the National Atmospheric Emission Inventory 2019. Retrieved from: https://naei.beis.gov.uk/reports/reports?report_id=1024.
van den Hove, A., Verwaeren, J., van den Bossche, J., Theunis, J., de Baets, B., 2019. Development of a land use regression model for black carbon using mobile monitoring data and its application to pollution-avoiding routing. *Environ. Res.*
Wai, T.H., Apte, J.S., Harris, M.H., Kirchstetter, T.W., Portier, C., Preble, C.V., Roy, A., Szpiro, A.A., 2022. Insights from application of a hierarchical spatio-temporal model to an intensive urban black carbon monitoring dataset. *Atmos. Environ.* 277.
Wen, Y., Wang, H., Larson, T.V., Kelp, M.M., Zhang, S., Wu, Y., Marshall, J.D., 2019. On-highway vehicle emission factors, and spatial patterns, based on mobile monitoring and absolute principal component score. *Sci. Total Environ.* 676, 242–251.
WHO. 2021. WHO global air quality guidelines [Online]. Available: https://www.who.int/publications/i/item/9789240034433 [Accessed 19 December 2022].
Wyche, Smallbone, Hama, Hofman, J., Stroobants, Roekens, Weijers, Panteliadis & Wyche, K. P. The spatio-temporal evolution of black carbon in the North-West 1 European ' air pollution hotspot ' 2 3. 2020.
Xiao, H.W., Xu, Y., Xiao, H.Y., 2023. Source apportionment of black carbon aerosols in winter across China. *Atmos. Environ.*
Yang, Y., Zhao, D., Huang, Y., Tian, P., Liu, D., Huang, M., He, H., Ding, D., Li, Y., Zhao, C., 2022. Effects of black carbon aerosol on air quality and vertical meteorological factors in early summer in Beijing. Sci. Total Environ.
Zhang, X., Stocker, J., Johnson, K., Fung, Y.H., Yao, T., Hood, C., Carruthers, D., Fung, J. C.H., 2022. Implications of mitigating ozone and fine particulate matter pollution in the guangdong-hong kong-macau greater bay area of china using a regional-to-local coupling model. *GeoHealth* 6.
Zhang, S., Wu, X., Zheng, X., Wen, Y., Wu, Y., 2021. Mitigation potential of black carbon emissions from on-road vehicles in China. *Environ. Pollut.* 278, 116746.
Zhong, J., Hood, C., Johnson, K., Stocker, J., Handley, J., Wolstencroft, M., Mazzeo, A., Cai, X., Bloss, W.J., 2021. Using task farming to optimise a street-scale resolution air quality model of the west midlands (UK). *Atmos.* 12, 983.
Zhong, J., Harrison, R.M., James Bloss, W., Visschedijk, A.J.H., Denier Van Der Gon, H.A. C., 2023a. Modelling the dispersion of particle number concentrations in the West Midlands, UK using the ADMS-Urban model. *Environ. Int.* 181, 108273.
Zhong, J., Hodgson, J.R., James Bloss, W., Shi, Z., 2023b. Impacts of net zero policies on air quality in a metropolitan area of the United Kingdom: towards world health organization air quality guidelines. *Environ. Res.*
Zhong, J., Stocker, J., Cai, X., Harrison, R.M., Bloss, W.J., 2024. Street-scale air quality modelling over the West Midlands, United Kingdom: effect of idealised traffic reduction scenarios. *Urban Clim.* 55, 101961.